

Model for Spherical Cavity Radii and Potential Functions of Sorbates in Zeolites

M. S. A. Baksh and R. T. Yang

Dept. of Chemical Engineering, State University of New York, Buffalo, NY 14260

A spherical pore model for calculating the zeolite cavity radius and the potential energy of interactions of noble gases (Ar, Kr, Xe) is presented. The model utilizes the gas adsorption isotherm and equates the free energy change upon adsorption to the potential energy of interaction of the gas molecules with the zeolite cavity. The results obtained for the cavity radius using Ar, Kr, and Xe adsorption isotherms are in excellent agreement with those of the cavity radius for 5A, 13X, and Y zeolites obtained from crystallographic data. Also, the average potential energies of interaction of these gases with the surface atoms of the zeolite cavities, calculated from the isotherms and the spherical pore model, compare reasonably well with the internal energies determined from the experimental heats of adsorption.

Introduction

The adsorption isotherms of gases on molecular sieve zeolites provide valuable information in determining molecular forces between the gas molecules and the adsorbent atoms. The various model equations for the adsorption of gases on zeolites have been reviewed by Yang (1987). However, these equations do not always predict the isotherms for adsorption of noble gases (Derrah and Ruthven, 1975; Rowley et al., 1976). In addition, the interaction of the gas molecules with the adsorbent atoms brings about some uncertainties as to the nature of the various forces operating at the molecular level (Sinanoglu and Pitzer, 1960). More recently, computer simulations have been made to elucidate the behavior of adsorbed molecules on solid surfaces. Rowley et al. (1976) performed computer simulations for molecules adsorbed on flat surfaces. The results from such simulations were then used in determining important parameters that are characteristic to a given gas-solid system.

Monte Carlo simulations (Stroud 1976; Metropolis et al., 1953; June et al., 1990) have been used to evaluate the adsorption isotherms and thermodynamic properties of various adsorbates in molecular sieves. In addition, Peterson et al. (1988) used the grand canonical Monte Carlo method or molecular dynamics method and mean field density functional theory to evaluate adsorption isotherms and phase transitions for a Lennard-Jones fluid in cylindrical pores. Woods et al. (1988) used a virial expansion and direct calculation of the partition functions in calculating thermodynamic and structural properties for fluids adsorbed in zeolite cavities. Adams

(1975) used a Monte Carlo simulation technique to calculate the equilibrium properties of fluids having "soft" pair potentials, while Kiselev et al. (1981) calculated the thermodynamic properties of various gases (Ar, Kr, Xe, O₂, N₂) adsorbed on 13X and Y zeolites via molecular statistical techniques.

Everett and Powl (1976) have calculated the potential energy profiles for atoms adsorbed in slit-like pores and showed the enhancement of the depth of the potential energy well over that for adsorption on a flat surface. Using a slit model, Horvath and Kawazoe (1983) provided a method for the calculation of effective pore-size distribution from the adsorption isotherms in molecular sieve carbon. The Horvath and Kawazoe model was later used by Venero and Chiou (1988) to characterize 5A and Y zeolites by gas adsorption at low pressures. Although the slit model used by Venero and Chiou is inappropriate for zeolites, these authors were able to obtain pore sizes that compared reasonably well with the molecular sieving properties of these zeolites.

Soto et al. (1981) modified the Lennard-Jones and Devonshire (1937) theory of liquids to calculate dispersion forces of noble gases in 5A and 13X zeolites via the configurational integral. These authors were able to calculate the cavity radius and the potential energy of interactions from the isotherms of noble gases. However, their approach produced results for the cavity radius that deviates from the cavity radius obtained from crystallographic data.

In this work, we have developed a spherical pore model, analogous to the slit model of Horvath and Kawazoe for cal-

culating the cavity radius of zeolites possessing identical spherical cavities (e.g., 5A, 13X and Y), and we show with the aid of the adsorption isotherms (Ar, Kr, Xe) how to calculate the potential energy profiles for noble gases adsorbed in 5A, 13X and Y zeolites. This approach is quite simple in comparison to other methods (e.g., Monte Carlo and molecular dynamics) that have been used for relating macroscopic properties to intermolecular forces in gas-solid systems.

Theory

Review of slit model

The slit-potential model of Everett and Powl (1976) is used frequently for adsorption in microporous carbon since the pores in such materials are slit-like. This model was later extended by Horvath and Kawazoe (1983) by assuming a slab geometry with the slit walls consisting of two infinite graphitic planes. Excellent reviews of these theories are available in Saito and Foley (1991) and Suzuki (1990). Only a brief outline is given here. Everett and Powl (1976) showed that the potential energy of interaction, ϵ , between one adsorbate molecule and two parallel lattice planes whose nuclei are at a distance L apart can be expressed via the Lennard-Jones potential as:

$$\epsilon = K\epsilon^* \left[-\left(\frac{\sigma}{z}\right)^4 + \left(\frac{\sigma}{z}\right)^{10} - \left(\frac{\sigma}{L-z}\right)^4 + \left(\frac{\sigma}{L-z}\right)^{10} \right] \quad (1)$$

where

$$\sigma = \left(\frac{2}{5}\right)^{1/6} d_0$$

and $K = 3.07$. A schematic for the slit pore (Saito et al., 1991) is given in Figure 1A.

In the case of more than one adsorbate molecules, the value of ϵ^* in Eq. 1 is:

$$\epsilon^* = \frac{3}{10} \left[\frac{N_a A_a + N_A A_A}{d_0^4} \right] \quad (2)$$

where the dispersion constants are given by the Kirkwood-Muller formalism as:

$$A_a = \frac{6mc^2\alpha_s\alpha_A}{\left(\frac{\alpha_s}{\chi_s}\right) + \left(\frac{\alpha_A}{\chi_A}\right)}$$

$$A_A = \frac{3}{2} (mc^2\alpha_A\chi_A)$$

By combining Eqs. 1 and 2, the potential function for the slit pore filled with adsorbate molecules can be written as:

$$\epsilon(z) = \frac{N_A A_A + N_a A_a}{2\sigma^4} \times \left[-\left(\frac{\sigma}{z}\right)^4 + \left(\frac{\sigma}{z}\right)^{10} - \left(\frac{\sigma}{L-z}\right)^4 + \left(\frac{\sigma}{L-z}\right)^{10} \right] \quad (3)$$

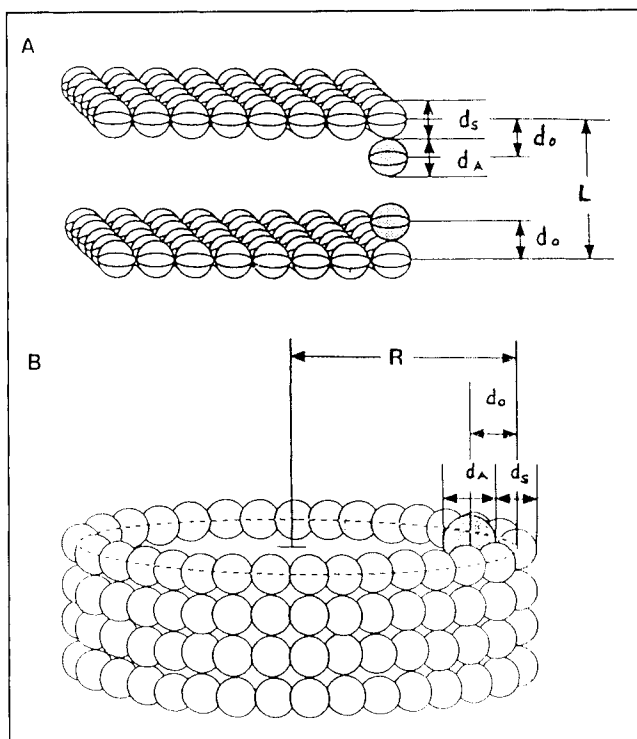


Figure 1. A, Slit-like pore geometry; B, cylindrical pore geometry.

The shaded circles, adsorbate atoms; open circles, oxygen atoms in the adsorbent surface
Courtesy of Saito and Foley (1991)

Horvath and Kawazoe (1983) used an energy balance and equated the free energy of adsorption to the net energy of interaction between the layers. Their result can be written as:

$$R_g T \ln(P/P_0) = N_{Av} \frac{\int_{d_0}^{L-d_0} \epsilon(z) dz}{\int_{d_0}^{L-d_0} dz} \quad (4)$$

Substituting Eq. 3 into Eq. 4, the Horvath and Kawazoe (1983) result for slit-like geometry becomes:

$$R_g T \ln(P/P_0) = N_{Av} \frac{N_A A_A + N_a A_a}{\sigma^4 (L - 2d_0)} \times \left[\frac{\sigma^4}{3(L-d_0)^3} - \frac{\sigma^{10}}{9(L-d_0)^9} - \frac{\sigma^4}{3d_0^3} + \frac{\sigma^{10}}{9d_0^9} \right] \quad (5)$$

Review of cylindrical model

In the case of cylindrical pores, Everett and Powl (1976) made the following assumptions:

- The cylindrical pore has finite radius (R) and infinite length (high aspect ratio, L/D).
- The inside wall of the cylinder is made up of a single layer of atoms (e.g., oxide atoms in the case of zeolites).

The results for the potential energy of interaction, $\epsilon(r)$,

between the adsorbate molecules and the inside wall of the cylinder are:

$$\epsilon(r) = \frac{5}{2} \pi \epsilon^* \left[\frac{21}{32} \left(\frac{d_0}{R} \right)^{10} \sum_{k=0}^{\infty} \alpha_k \left(\frac{r}{R} \right)^{2k} - \left(\frac{d_0}{R} \right)^4 \sum_{k=0}^{\infty} \beta_k \left(\frac{r}{R} \right)^{2k} \right] \quad (6)$$

$$\alpha_k^{1/2} = \frac{\Gamma(-4.5)}{\Gamma(-4.5-k)\Gamma(k+1)} \quad (7)$$

and

$$\beta_k^{1/2} = \frac{\Gamma(-1.5)}{\Gamma(-1.5-k)\Gamma(k+1)} \quad (8)$$

where R denotes the radius of the cylinder (see Figure 1B), ϵ^* as defined in Eq. 2, and r represents the distance of the gas molecule from the central axis of the cylinder. Saito and Foley (1991) assumed that adsorption occurs only on the inside wall of the cylinder in the micropore region, and the interactions upon adsorption are approximated by the interactions between the gas molecules and the solid (adsorbent). By equating the free energy of adsorption to the average intermolecular potential in the cylindrical pore, and using an area average defined as:

$$\bar{\epsilon} = \frac{\int_0^{2\pi} \int_0^{R-d_0} \epsilon(r) r dr d\theta}{\int_0^{2\pi} \int_0^{R-d_0} r dr d\theta} \quad (9)$$

Saito and Foley (1991) obtained the following cylindrical pore model result:

$$R_g T \ln \left(\frac{P}{P_0} \right) = \frac{3}{4} \pi N_{Av} \frac{(N_A A_A + N_v A_s)}{d_0^4} \times \sum_{k=0}^{\infty} \left[\frac{1}{(k+1)} \left(1 - \frac{d_0}{R} \right)^{2k} \left(\frac{21}{32} \alpha_k \left[\frac{d_0}{R} \right]^{10} - \beta_k \left[\frac{d_0}{R} \right]^4 \right) \right] \quad (10)$$

Now we proceed to the development of the spherical pore model that is appropriate for zeolites possessing identical spherical cavities.

Spherical pore model

The atoms and ions forming the walls of the cavities in 5A, 13X and Y zeolites lie in polyhedral shells that may be approximated by spheres. Also, these zeolites can be considered to be a collection of identical cavities (Breck, 1974; Brousard and Shoemaker, 1960). The adsorption of gases in these zeolites can be considered as sorption in spherical cavities. And, the free energy of adsorption can be related to the energy of interaction of the adsorbate molecules with the walls of the zeolite cavities. Since these zeolites possess identical spherical cavities, the model equations are developed using one spherical cavity. The steps in developing the model equations are as follows:

- The potential function is derived for one adsorbate molecule interacting with the atoms in the wall of the zeolite cavity.

- The relationship between the free energy of adsorption and the potential function is determined. This step will give the result analogous to Eq. 4, which upon integration will give an equation corresponding to Eq. 5 or 10.

- The results in the previous steps are used in conjunction with the isotherm and the Lennard-Jones potential function to determine the final equations.

The first step is the most difficult; however, the problem is simplified tremendously by making the following assumptions:

- All the surface atoms of the cavity wall are located at the same distance from the center of the cavity.

- The interaction between the gas molecule with the atoms of the cavity wall can be represented by the Lennard-Jones 12:6 potential.

- The dispersion and repulsive contributions to the potential energy can be considered spherically symmetric. Thus, the atoms of the cavity can be replaced by a uniform, continuous distribution of centers of force, and the summation of pair potentials can be replaced by integration. Such an approximation resulted in < 10% error as revealed by Soto et al. (1981).

The Lennard-Jones 12:6 potential can be written as:

$$\Gamma_{12} = 4\epsilon_{12}[(\sigma/r)^{12} - (\sigma/r)^6] \quad (11)$$

where Γ_{12} is the Lennard-Jones 12:6 potential for the interaction between molecular species of 1 and 2. The interactions between the zeolite cavity wall, consisting of a single lattice plane (SLP), and a single adsorbate molecule of 1 in the gas phase, a distance $(R-z)$ from the curve-plane of surface nuclei is obtained readily by integrating Eq. 11 over the cavity internal surface. Thus,

$$\Gamma_{1,SLP} = \int_0^{2\pi} \int_0^{\pi} n_e \Gamma_{12}(z, \theta) R^2 \sin \theta d\theta d\phi \quad (12)$$

where R is the cavity radius, z is the radial distance of the

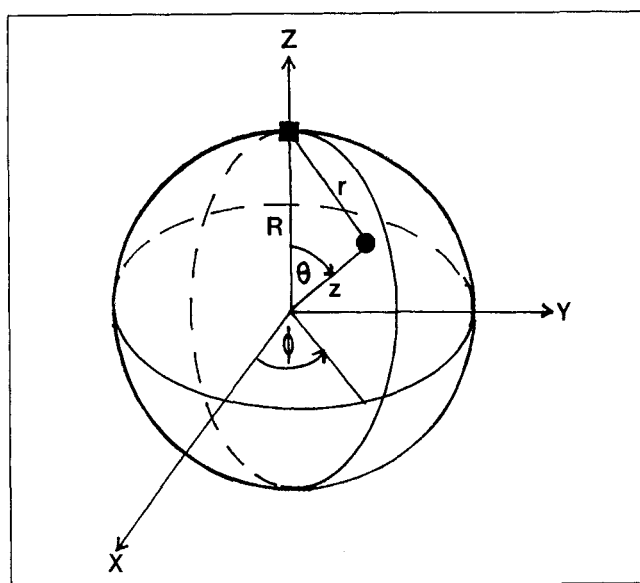


Figure 2. Spherical pore geometry.

adsorbate molecule from the center of the cavity (see Figure 2), and n_e is the number of oxygen atoms per unit area on the cavity surface. We have implicitly assumed in Eq. 12 that only oxygen atoms on the surface of the cavity wall interact with the gas molecule. According to Kiselev (1985), the framework silicon/aluminum atoms do not interact significantly with the adsorbate molecules, since the adsorbate molecule is surrounded by a latticework of framework oxygen atoms, and the silicon/aluminum atoms located at the centers of $\text{SiO}_4/\text{AlO}_4$ tetrahedra are more recessed from the center of the zeolite cavity, giving negligible contribution to the total potential energy. In addition, we rely on our model regression parameters to correct for such an approximation. Substituting Eq. 11 into Eq. 12, eliminate r using

$$r^2 = R^2 + z^2 - 2Rz \cos \theta$$

(see Figure 2) and carrying out the integration gives the potential energy of one adsorbate molecule interacting with the atoms of the cavity wall. The resulting equation is:

$\Gamma_{1,SLP}$

$$= (8\pi R^2 n_e \epsilon_{1s}) \left[- \left(\frac{\sigma_{1s}}{R} \right)^6 \frac{1}{4(z/R)} \left(\frac{1}{(1-z/R)^4} - \frac{1}{(1+z/R)^4} \right) + \left(\frac{\sigma_{1s}}{R} \right)^{12} \frac{1}{10(z/R)} \left(\frac{1}{(1-z/R)^{10}} - \frac{1}{(1+z/R)^{10}} \right) \right] \quad (13)$$

Equation 13 can be written in the following alternative form:

$$\Gamma_{1,SLP} = 4N\epsilon_{1s} \left[\left(\frac{\sigma_{1s}}{R} \right)^{12} L(z^2/R^2) - \left(\frac{\sigma_{1s}}{R} \right)^6 M(z^2/R^2) \right] \quad (14)$$

where

$$L(z^2/R^2) = \frac{1 + 12(z^2/R^2) + 25.2(z^2/R^2)^2 + 12(z^2/R^2)^3 + (z^2/R^2)^4}{(1 - z^2/R^2)^{10}} \quad (15)$$

and

$$M(z^2/R^2) = \frac{1 + z^2/R^2}{(1 - z^2/R^2)^4} \quad (16)$$

Equation 13 or Eqs. 14–16 correspond to the Lennard-Jones and Devonshire (1937) results that were obtained from the cell theory of fluids.

Now we proceed to the second step in the model development. The net energy of interaction (Γ_{net}) inside the zeolite cavity is given by:

$$\Gamma_{\text{net}} = \frac{\int_0^{R-d_0} \Gamma_{1,SLP}(z) 4\pi z^2 dz}{\int_0^{R-d_0} 4\pi z^2 dz} \quad (17)$$

where $\Gamma_{1,SLP}$ is given by Eq. 13 or Eq. 14–16, and Figure 2 shows the geometry and the various parameters of the spherical pore, where d_0 is defined as:

$$d_0 = \frac{1}{2} (d_s + d_A) \quad (18)$$

Substituting Eq. 13 into Eq. 17 and performing the integration give:

$$\Gamma_{\text{net}} = \frac{6N\epsilon_{1s}R^3}{(R-d_0)^3} \left[- \left(\frac{\sigma_{1s}}{R} \right)^6 \left(\frac{1}{12} T_1 + \frac{1}{8} T_2 \right) + \left(\frac{\sigma_{1s}}{R} \right)^{12} \left(\frac{1}{90} T_3 + \frac{1}{80} T_4 \right) \right] \quad (19)$$

$$T_1 = \frac{1}{\left(1 - \frac{R-d_0}{R}\right)^3} - \frac{1}{\left(1 + \frac{R-d_0}{R}\right)^3} \quad (20)$$

$$T_2 = \frac{1}{\left(1 + \frac{R-d_0}{R}\right)^2} - \frac{1}{\left(1 - \frac{R-d_0}{R}\right)^2} \quad (21)$$

$$T_3 = \frac{1}{\left(1 - \frac{R-d_0}{R}\right)^9} - \frac{1}{\left(1 + \frac{R-d_0}{R}\right)^9} \quad (22)$$

$$T_4 = \frac{1}{\left(1 + \frac{R-d_0}{R}\right)^8} - \frac{1}{\left(1 - \frac{R-d_0}{R}\right)^8} \quad (23)$$

Equations 19–23 can be written in the following alternative form:

$$\Gamma_{\text{net}} = N\epsilon_{1s} \left(\frac{R}{R-d_0} \right)^2 \times \left[- \left(\frac{\sigma_{1s}}{R} \right)^6 (M_1 - M_2) + \left(\frac{\sigma_{1s}}{R} \right)^{12} (L_1 - L_2) \right] \quad (24)$$

where the equations for M_1 and M_2 are given by:

$$M_1 = \frac{3 + \left(\frac{R-d_0}{R} \right)^2}{\left(1 - \left(\frac{R-d_0}{R} \right)^2\right)^3} \quad (25)$$

$$M_2 = \frac{3}{\left(1 - \left(\frac{R-d_0}{R} \right)^2\right)^2} \quad (26)$$

and the equations for L_1 and L_2 by:

$$L_1 = \frac{6}{5} \left[\frac{1 + \frac{28}{3} \left(\frac{R-d_0}{R} \right)^2 + 14 \left(\frac{R-d_0}{R} \right)^4 + 4 \left(\frac{R-d_0}{R} \right)^6 + \frac{1}{9} \left(\frac{R-d_0}{R} \right)^8}{\left(1 - \left(\frac{R-d_0}{R} \right)^2 \right)^9} \right] \quad (27)$$

$$L_2 = \frac{6}{5} \left[\frac{1 + 7 \left(\frac{R-d_0}{R} \right)^2 + 7 \left(\frac{R-d_0}{R} \right)^4 + \left(\frac{R-d_0}{R} \right)^6}{\left(1 - \left(\frac{R-d_0}{R} \right)^2 \right)^8} \right] \quad (28)$$

The collision diameter, σ_{1s} , appearing in Eq. 24 is defined as:

$$\sigma_{1s} = \frac{1}{2} [\sigma_{11} + \sigma_{ss}] \quad (29)$$

If the free energy of adsorption is equated to the net energy of interaction between the adsorbate molecules and the atoms of the zeolite cavities, the energy balance yields:

$$\ln \frac{P}{P_0} = \left([1,000/q] \frac{\eta}{R_g T} N_{\epsilon_{1s}} \right) \left(\frac{R}{R-d_0} \right)^2 \Gamma_{\text{net}} \quad (30)$$

where q is the amount adsorbed in mmol/g, η is the number of cavities in one gram of zeolite, and Γ_{net} is given by Eqs. 24–28. If we treat q (mmol/g) as the independent variable, and $\ln(P/P_0)$ as the dependent variable, we can use the isotherm data of the adsorbate to solve for the two unknowns, namely

$$1,000 \frac{\eta}{R_g T} N_{\epsilon_{1s}}, \text{ and the cavity radius } (R)$$

A nonlinear least square regression algorithm was used to determine these two unknowns; and since the values of η are known for 5A, 13X, and Y zeolites, the values of $N_{\epsilon_{1s}}$ are calculated for each of the adsorbates. These values are then used in Eqs. 14–16 to compute the potential energy functions of the various adsorbates in the zeolite cavities. In addition, the average potential energies can be calculated readily from Eqs. 24–29.

Adsorption Isotherms

The adsorption isotherms of noble gases (Ar, Kr, and Xe) on 5A, 13X and Y zeolites were used to illustrate the usefulness of the spherical pore model in calculating the cavity radius and

the potential energy function. The isotherms were taken from the literature. The isotherms of argon on 5A and Y zeolites at 87.5 K were obtained from Venero and Chiou (1988). The isotherms for Kr on 5A zeolite at 195 K from Mahajan and Walker (1969), and on 13X zeolite at 203 K from Rees and Williams (1964). The isotherm for Xe at 213 K on 13X zeolite was taken from Aristov et al. (1966). Some of the isotherms were given as the amount adsorbed as a function of pressure, whereas $\ln(P/P_0)$ is given in Eq. 30; therefore, one must estimate the vapor pressures for some of the adsorbates at the adsorption temperatures. The Riedel correlation (Reid and Sherwood, 1958) was used to estimate the vapor pressures of the noble gases. The single-constant reduced-vapor pressure equation is:

$$\log_{10} \left(\frac{1}{P_r} \right) = \Phi(T_r) + (\alpha - 7)\psi(T_r) \quad (31)$$

where

$$\Phi(T_r) = 0.118\gamma(T_r) - 7\log_{10} T_r \quad (32)$$

$$\psi(T_r) = 0.0364\gamma(T_r) - \log_{10} T_r \quad (33)$$

$$\gamma(T_r) = \frac{36}{T_r} + 42\ln T_r - 35 - T_r^6 \quad (34)$$

In applying the Riedel correlation using Eqs. 31–34, the constant α was calculated first using data of the normal boiling

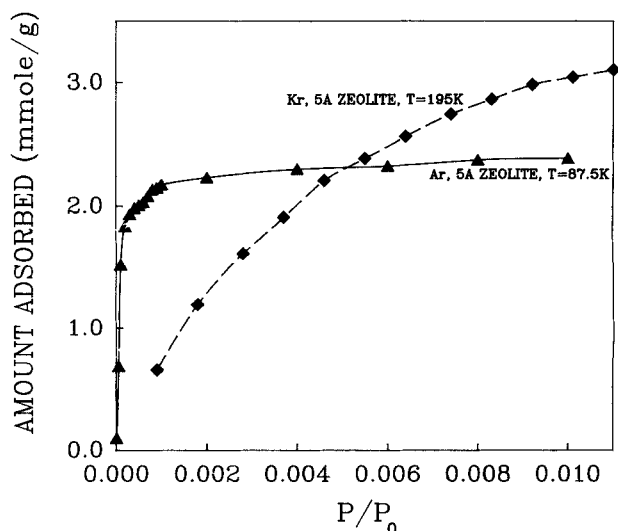


Figure 3. Adsorption isotherms of noble gases on 5A zeolite.

Table 1. Physical Properties of Noble Gases and Parameter Values for Eqs. 31–34

Adsorbate	T_{nbp} K	T_c K	P_c atm	T_r	$\gamma(T_r)$	$\psi(T_r)$	P_0 atm
Ar	87.5	150.7	48.0	0.581	2.138	0.386	1.0
Ar	87.5	150.7	48.0	0.581	2.138	0.386	1.0
Kr	120.7	195	54.3	0.932	0.216	0.031	35.77
Kr	120.7	195	54.3	0.970	0.093	0.013	45.33
Xe	165.9	289.6	58.0	0.736	1.036	0.165	8.173

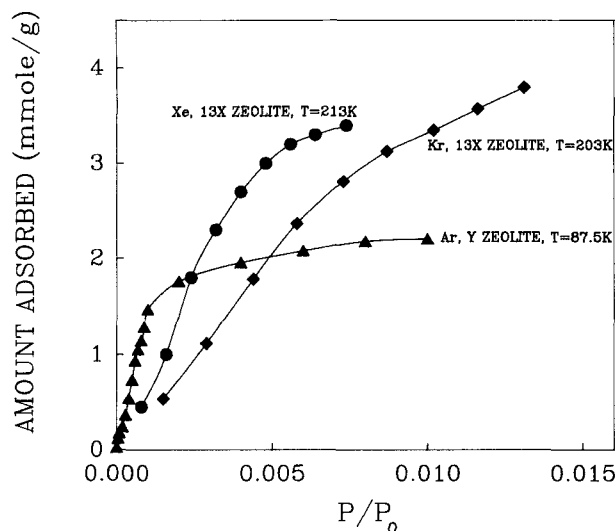


Figure 4. Adsorption isotherms of noble gases on 13X and Y zeolites.

point of each adsorbate. Then, the vapor pressures at other temperatures were readily calculated. The results from the Riedel correlation are summarized in Table 1. Also included in the table are the physical properties of argon, krypton and xenon used in the calculations. Once the vapor pressure at the adsorption temperature for each of the adsorbates was determined, the corresponding isotherms were replotted to enhance usability. The replotted isotherms are displayed in Figures 3 and 4.

The collision diameter σ_{1s} in Eq. 24 was estimated from Eq. 29, where the subscript 1 refers to the adsorbate molecule, and the subscript s to the oxygen atom in the cavity wall. From crystallographic data of Brousard and Shoemaker (1960), the average distance between the oxygen atoms in the cavities of 5A and 13X zeolites is 0.276 nm, and this value was used for σ_{ss} . The values of η , the number of cavities per gram of zeolite (5A, 13X, Y), are given by Breck (1974), which are listed in Table 2. The values σ_{11} for the noble gases are listed in Table 3.

Results and Discussion

The results obtained from a nonlinear least square regression algorithm in solving Eq. 30 are given in Tables 2-3. In Table 2, the cavity radius was determined using different adsorbates and Eq. 30. The results indicated no preference for any of the adsorbates used in the calculation of the cavity radius. In addition, the cavity radius obtained from the spherical pore model is in excellent agreement with the results of 0.7040 nm

Table 2. Cavity Parameters for Molecular Sieves 5A, 13X and Y Zeolites, Spherical Pore Model*

	5A	13X	Y
R , cavity radius, nm	0.70 (Ar)	0.70 (Kr)	0.71 (Ar)
R , cavity radius, nm	0.71 (Kr)	0.71 (Xe)	—
η , cavities/g	3.59×10^{20}	3.64×10^{20}	3.64×10^{20}
σ_{ss} , nm	0.276	0.276	0.276

*The adsorbates used in calculating cavity radius for various gas-solid systems are indicated in the parentheses.

Table 3. Potential Energy Parameters for Gases Adsorbed in Molecular Sieves 5A, 13X and Y Zeolites: Spherical Pore Model

Adsorbate	σ_{11} (nm)	$N_{e_{1s}}/k$ (K)		
		5A	13X	Y
Ar	0.335	27,244	—	17,586
Kr	0.357	33,734	23,320	—
Xe	0.390	—	22,647	—

and 0.7057 nm reported for zeolites 5A and 13X, respectively (Breck, 1974; Brousard and Shoemaker, 1960).

The potential energies for the noble gases interacting with the zeolite cavities (5A, 13X, and Y) were calculated using Eqs. 14-16 with the values of $N_{e_{1s}}$ obtained from the spherical pore model. The results obtained for the potential energies are displayed in Figures 5-6.

The advantage of calculating potential energies of interaction in zeolite cavities via the spherical pore model is to avoid the necessity of using the formulae that are frequently used for evaluating the dispersion constants. Derrah and Ruthven (1975) have used the Kirkwood-Muller, Slater-Kirkwood, and London formulae to estimate the potential energy functions of noble gases in 5A zeolite. They have shown that the choice of the various formulae produced quite different energy profiles, and they concluded that for Kr and Xe, the Slater-Kirkwood formula gives the best agreement with experimental data, while the London formula works best for Ar. According to Walker (1966), there is difficulty in deciding which formulae to accept in calculating the dispersion constants, but the most frequently used are those by Slater-Kirkwood, Kirkwood-Muller, London, Bardeen, and Margenau and Pollard. Generally, the London formula gives the lower limit of σ values, whereas the Kirkwood-Muller expression yields the upper limit of σ values.

Consequently, the calculated energy profiles obtained with these different formulae are quite different and sometimes incorrect. In addition, the choice of which formula to use in

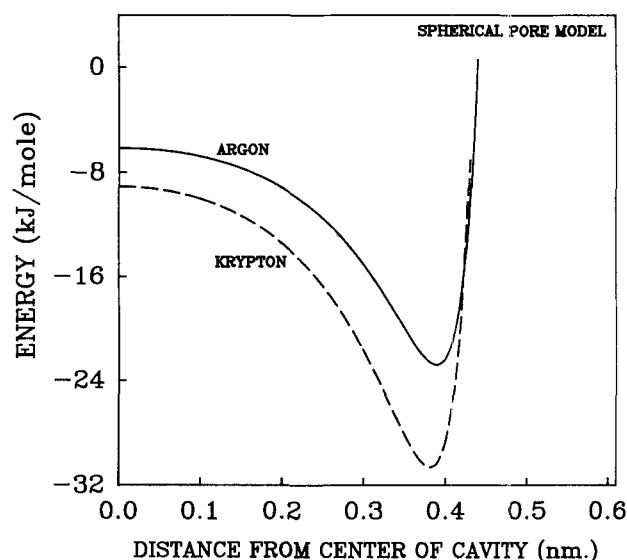


Figure 5. Potential energy for noble gases interacting with 5A zeolite cavity.

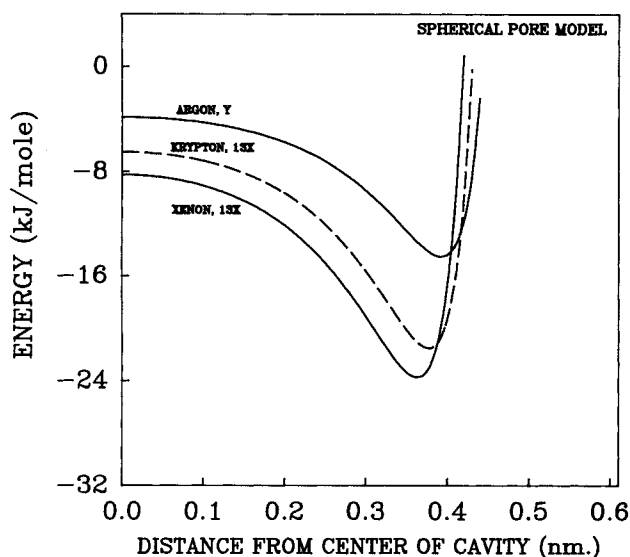


Figure 6. Potential energy for noble gases interacting with zeolite 13X and Y cavities.

evaluating dispersion constants could be dictated by the availability of experimental data for a given adsorbate/adsorbent system. For example, in using the London formula, the ionization potentials and the polarizabilities of the adsorbate and the adsorbent must be available. Thus, the selection of the formula could be reduced to the availability of experimental data, which could produce erroneous results for the potential energy profiles.

The energy profiles of Figures 5–6 show a shift in the location of the energy minimum for the different gases. Xenon, having the largest molecular size compared to argon and krypton, will experience repulsive force much earlier than Ar and Kr when approaching the wall surface. Thus, argon can approach the cavity wall much closer than xenon. Therefore, the potential energy well for xenon is furthest from the cavity wall or closest to the center of the zeolite cavity.

Walker (1966) suggested that the minima in the potential energy profiles (Figures 5–6) should correspond closely to the heats of adsorption at very low coverage (<0.3). However, since the average potential energies are measured by ΔU (Derah and Ruthven, 1975), a comparison between the volume-average potential energies and the experimental ΔU values seems more appropriate. The volume-average potential energies and the potential energy minima obtained via the spherical pore model are given in Table 4. Also included in the table are the ΔU values calculated from the experimental heats of adsorption (Ruthven et al., 1975; Kiselev et al., 1981). In calculating ΔU from heats of adsorption, we used

$$-\Delta H = -\Delta U + R_g T \quad (35)$$

There are noticeable differences between the average potential energies and the ΔU values. The differences could be attributed to using incorrect values for the heats of adsorption. For example, Rees et al. (1964) have shown that for krypton adsorption on 13X zeolite, the heat of adsorption has a value of about 16.74 kJ/mol for coverage less than 0.4. However, at coverage larger than 0.4, a substantial increase in the heat of adsorption was observed ($>10\%$). Also, these authors (Rees

Table 4. Calculated Average Potential Energies and Energy Minima from Spherical Pore Model vs. ΔU Values from Experimental Heats of Adsorption (ΔH) by Eq. 35

Adsorbate	Adsorbent	Energy Minima (kJ/mol)	Avg. Energy (kJ/mol)	ΔU (Exp.) (kJ/mol)
Ar	5A	-22.81	-16.03	-13.33*
Kr	5A	-30.63	-21.48	-16.12*
Ar	Y	-14.53	-10.17	-8.61**
Kr	13X	-21.52	-15.71	-13.80**
Xe	13X	-23.72	-17.76	-19.2**

*Ruthven et al. (1975)

**Kiselev et al. (1981)

et al.) have indicated that the heat of adsorption determined at low coverage increased as the temperature decreased.

In addition, the experimental ΔU values listed in Table 4 were obtained from isotherms at low coverage (<0.3), while isotherms spanning a larger range of coverage were used in the spherical pore model. However, if the values for ΔU were obtained from isotherms spanning a larger range of coverage, a closer agreement between average potential energies and ΔU values could be obtained. According to Rees et al. (1964), more than 10% increase in the ΔU value was observed for krypton interacting with 13X zeolite for coverage larger than 0.4. These complications made it very difficult to accurately compare the average energies in the potential energy profiles with ΔU values obtained from heats of adsorption data at different coverages and from isotherms at various temperatures. In addition, the assumptions made in the derivation of the spherical pore model may partially account for the differences between the average potential energies and ΔU values. Nevertheless, the differences are not too excessive for some gas/solid systems (Ar/Y, Kr/13X, and Xe/13X). For example, in the case of Xe/13X, the difference between the average potential energy and the internal energy (ΔU) is less than 8%. However, for Kr/5A, the error is quite large (about 33%). To make a fair comparison between the internal energies and the average potential energies, it is suggested that the isotherms used in the spherical pore model be used in the calculation of the heats of adsorption. Also, additional isotherms needed for the calculation of the heats of adsorption be at temperatures that are not very different (within 100 degrees).

It is obvious from Table 4 that for a given adsorbent, the energy minimum increases as the size of the adsorbate molecule increases. Therefore, we should expect the ΔU value on a given adsorbent to increase with increasing adsorbate size. By comparing the ΔU values (Table 4) for the Ar/Y, Kr/13X, and Xe/13X systems, we noted that the ΔU value increases with increasing adsorbate size, which is consistent with the calculated energy minima displayed in Figure 6.

Acknowledgment

This work was supported by the NSF under grant CTS-8914754.

Notation

- A = dispersion constant
- c = speed of light
- d = diameter of an atom

d_0 = arithmetic mean of diameters of the adsorbate and adsorbent
 $-\Delta H$ = differential molar heat of adsorption
 L = distance between the nuclei of two parallel layers in slit-like pore
 m = mass of an electron
 N = number of oxygen atoms in the surface of zeolite cavity
 N_{Av} = Avogadro's number
 n_o = number of oxygen atoms per unit area in cavity surface
 P = pressure
 P_0 = saturated vapor pressure of adsorbate
 q = amount adsorbed, mmol/g
 r = distance between gas molecule and cylinder's central axis (cylindrical model) or gas molecule and oxygen atom in the spherical cavity wall (spherical pore model)
 R = zeolite cavity radius
 R_g = gas constant
 T = absolute temperature
 $-\Delta U$ = differential molar internal energy
 z = distance of adsorbate molecule from the cavity center in spherical pore model or from a surface atom in the slit layer for slit model

Greek letters

ϵ = potential energy of interaction in slit or cylindrical pore
 α = polarizability
 χ = magnetic susceptibility
 Γ = potential energy of interaction in zeolite cavity
 σ_{1s} = distance from an atom at zero interaction energy
 η = number of cavities per gram of zeolite
 θ = angle in spherical coordinate system, $0 \leq \theta \leq \pi$
 ϕ = angle in spherical coordinate system, $0 \leq \phi \leq 2\pi$

Subscripts

A = adsorbate
 s = adsorbent

Literature Cited

- Adams, D. J., "Grand Canonical Ensemble Monte Carlo for a Lennard-Jones Fluid," *Molec. Phys.*, **29**(1), 307 (1975).
- Aristov, B. G., V. Bosacek, and A. V. Kiselev, "Dependence of Adsorption of Krypton and Xenon by Crystals of Zeolite LiX and NaX on Pressure and Temperature," *Farad. Soc. Trans.*, **63**, 2057 (1967).
- Breck, D. W., *Zeolite Molecular Sieves*, Wiley, New York (1974).
- Broussard, L., and D. P. Shoemaker, "The Structure of Synthetic Molecular Sieves," *J. ACS*, **82**, 1041 (1960).
- Derrah, R. I., and D. M. Ruthven, "Sorption of Inert Gases (Ar, Kr, and Xe) in Type A Zeolites," *Can. J. Chem.*, **53**, 996 (1975).
- Everett, H. D., and J. C. Powl, "Adsorption in Slit-like and Cylindrical Micropores in the Henry's Law Region," *J. Chem. Soc. Farad. Trans.: I*, **72**, 619 (1976).
- Horvath, G., and K. Kawazoe, "Method for the Calculation of Effective Pore Size Distribution in Molecular Sieve Carbon," *J. Chem. Eng. Japan*, **16**(6), 470 (1983).
- June, R. L., A. T. Bell, and D. N. Theodorou, "Prediction of Low Occupancy Sorption of Alkanes in Silicalite," *J. Phys. Chem.*, **94**(4), 1508 (1990).
- Kiselev, A. V., A. A. Lopatkin, and A. A. Shulga, *Zeolites*, **5**, 261 (1985).
- Kiselev, A. V., and P. Q. Du, "Molecular Statistical Calculation of the Thermodynamic Adsorption of Zeolites using the Atom-Atom Approximation," *J. Chem. Soc. Farad. Trans.: II*, **77**, 17 (1981).
- Lennard-Jones, J. E., and A. F. Devonshire, "Critical Phenomena in Gases—I," *Proc. Roy. Soc. (London) A*, **163**, 53 (1937).
- Mahajan, O. P., and P. L. Walker, Jr., "Krypton Adsorption on Microporous Carbons and 5A Zeolites," *J. Colloid and Interf. Sci.*, **29**(1), 129 (1969).
- Metropolis, N., A. W. Rosenbluth, M. N. Rosenbluth, A. H. Teller, and E. Teller, "Equation of State Calculations by Fast Computing Machines," *J. Chem. Phys.*, **21**, 1087 (1953).
- Peterson, B. K., K. E. Gubbins, G. S. Heffelfinger, U. M. B. Marconi, and F. V. Swol, "Lennard-Jones Fluids in Cylindrical Pores: Non-local Theory and Computer Simulation," *J. Chem. Phys.*, **88**(10), 6487 (1988).
- Rees, L. V. C., and C. J. Williams, "Sorption of Krypton in Linde Molecular Sieve 13X," *Farad. Soc. Trans.*, **60**, 1973 (1964).
- Reid, R. C., and T. K. Sherwood, *The Properties of Gases and Liquids: Their Estimation and Correlation*, McGraw-Hill, New York (1958).
- Rowley, L. A., D. Nicholson, and N. G. Parsonage, "Grand Ensemble Monte Carlo Studies of Physical Adsorption I—Results for Multilayer Adsorption of 12:6 Argon in the Field of a Plane Homogeneous Solid," *Molec. Phys.*, **31**, 365 (1976).
- Rowley, L. A., D. Nicholson, and N. G. Parsonage, "Grand Ensemble Monte Carlo Studies of Physical Adsorption II—the Structure of the Adsorbate: Critique of Theories of Multilayer Adsorption of 12-6 Argon on a Plane Homogeneous Solid," *Molec. Phys.*, **31**, 389 (1976).
- Ruthven, D. M., and R. I. Derrah, "Diffusion of Monatomic and Diatomic Gases in 4A and 5A Zeolites," *Farad. Trans.: I*, **71**, 2031 (1975).
- Saito, A., and H. C. Foley, "Curvature and Parametric Sensitivity in Models for Adsorption in Micropores," *AIChE J.*, **37**(3), 429 (1991).
- Sinanoglu, O., and K. S. Pitzer, "Interactions between Molecules Adsorbed on a Surface," *J. Chem. Phys.*, **32**, 1279 (1960).
- Soto, L. J., P. W. Fisher, A. J. Glessner, and A. L. Myers, "Sorption of Gases in Molecular Sieves—Theory for Henry's Constant," *J. Chem. Soc. Farad. Trans.: I*, **77**, 157 (1981).
- Stroud, H. J. F., E. Richard, P. Limcharoen, and N. G. Parsonage, "Thermodynamic Study of Linde Sieve 5A + Methane System," *J. Chem. Soc. Farad.: I*, **72**, 942 (1976).
- Suzuki, M., *Adsorption Engineering*, Elsevier, New York (1990).
- Venero, A., and J. N. Chiou, "Characterization of Zeolites by Gas Adsorption at Low Pressures," *Mat. Res. Soc. Symp. Proc.*, **111**, 235 (1988).
- Walker, P. L., "Chemistry and Physics of Carbon," *A Series of Advances*, Walker, P. L., ed., **2**, Marcel Dekker, New York (1966).
- Woods, B. G., A. Z. Panagiotopoulos, and J. S. Rowlinson, "Adsorption of Fluids in Model Zeolite Cavities," *Molec. Phys.*, **63**(1), 49 (1988).
- Yang, R. T., *Gas Separation by Adsorption Processes*, Butterworth, Boston (1987).

Manuscript received Jan. 15, 1991, and revision received Mar. 21, 1991.